MATHEMATICAL AND COMPUTER MODELING OF CRITICAL AREAS OF LOSS OF STABILITY OF COMPLEX SYSTEMS

KULSHAT AKANOVA,[1] ASSEM MYRKANOVA,[2] ANAR ZHUMAKHANOVA[3]

[1,2,3] Mathematical and computer modeling Department. L.N.Gumilyov Eurasian National University.

Kazakhstan

E-mail: [1]assema80@bk.ru, [2]akanova_km@mail.ru, [3]zhumanar@gmail.com

ABSTRACT

In recent years, the pace and scale of the development of minerals and energy resources in mountainous areas has been increasing, so various ground and underground structures are being built and operated. Increasing anthropogenic load on the biosphere and technosphere leads to the intensification of natural and man-made disasters. In addition, the occurrence of a catastrophe of the first type can provoke the manifestation of a catastrophe of the second type, and vice versa. Using ideas about catastrophic phenomena and the dynamics of their development, rock mechanics and methods of mathematical and computer modeling, it became possible to apply theoretical knowledge in practice. The issues of forecasting, preventing and minimizing events leading to loss of life and economic damage are among the most relevant today [1].

The article shows a study of the stress-strain state of an underground tunnel, which is affected by the volumetric weight of a rock mass. Deformation and displacement of mountain ranges can lead to the loss of stability of the technical structure and to its collapse, and thus cause a man-made disaster. The analytical and numerical solution of the problem will allow engineers and specialists in the field of mining to improve the safety and reliability of underground structures and take preventive measures to prevent the risk of their destruction. In this article, formulas are obtained for determining the components of stresses, deformations and displacements in an untouched rock mass, as well as on the contour of a constructed underground structure at bifurcation points. With their help, zones of high concentration of stresses, deformations and displacements and changes in the nature of their distribution are identified, which signal a critical state of the system, in which it can lose stability. As an example, an underground working of an elliptical profile is considered.

Keywords: *Stress, Deformation, Collapse, Bifurcation, Catastrophe.*

1. INTRODUCTION

Complex dynamic mechanical, ecological, technical and other systems can be in both unstable and stable states. The study of instability problems is carried out with the help of the theory of bifurcations and catastrophes.

The issues of modeling natural disasters are considered in the work of scientists S.L. Castillo Daza and F. Naranjo Mayorga [1]. Problems of the theory of stability and bifurcations of various systems are reflected in the works of G. Whitney and A. Poincaré, A. to a smooth change in external conditions" [2].

In unstable systems, there is such a phenomenon as bifurcation.

Lyapunov [3]. Then, in their works, Gilmore R. [4] and Zhang W. [5,6] carried out a deep classification of catastrophe and bifurcation models. The risks of disasters lead to various material and socio-economic damage, so the study of the precursors of their occurrence is an important task [7].

Arnold V.I. gives the following definition: "Disasters are called spasmodic changes that occur in the form of a sudden response of the system

Bifurcation is a process when a stable equilibrium of a system can become unstable when parameters change, and a continuous process can

become discontinuous over time [8]. In this case, a critical change in the system can occur with minor changes in external influences. Then the system at the bifurcation point continues to develop not along the old trajectory, but jumps over to a new trajectory far from equilibrium, and then this process can be repeated.

Bifurcations are classified as soft and hard [9].

A soft bifurcation is a transition from one stable state to another, while the new stable state does not have significant qualitative differences from the original one.

devices and structures under the conditions of man-made disasters, in which they can experience destruction deformations [10].

When designing and building structures, ensuring their stability is the main task, therefore, it is necessary to conduct a quantitative and qualitative assessment of the state of the mountain range. The use of graphic design tools and a package of applied programs during calculations will increase the accuracy of calculations and provide convenient visualization of the results.

2. STATEMENT OF THE PROBLEM AND METHODS FOR ITS SOLUTION

Formulation of the problem.

Let an underground tunnel with a non-circular profile be built in an untouched mountain range. It is required to find the components of the stress and strain vector in the rock mass in the vicinity of such a structure, under which its stability is lost, which can lead to a man-made disaster.

The stress state of an elastic plane with a hole consists of the components of the main stresses of a rock mass without a hole, and the components of additional stresses due to the presence of a hole. Then the stress functions can be represented as a sum about formula (1):
on to the problem of determining the components of stresses and displacements in the vicinity of a horizontal construction.

Let us place the origin of the Cartesian coordinate system in the center of the proposed underground structure and write down the equations of the plane theory of elasticity. We represent the equilibrium equations for the initial main untouched state of the rock mass in the form of expression (3):

$$\frac{\partial \sigma_x^0}{\partial x} + \frac{\partial \tau_{yx}^0}{\partial y} = 0; \quad \frac{\partial \tau_{xy}^0}{\partial x} + \frac{\partial \sigma_y^0}{\partial y} = 0; \quad \tau_{xy}^0 - \tau_{yx}^0 = 0 \qquad (3)$$

A rigid bifurcation is a bifurcation, as a result of which the system acquires a qualitatively new stable state, not similar to the original one. It is the rigid bifurcations that formed the basis of the theory of catastrophes.

Seismotectonic activity of the rock mass, anisotropy and heterogeneity of the properties of the environment, the influence of other geomechanical factors cause spatial changes in deformations and stresses in underground and surface engineering structures. Of great importance in science and technology are the properties of reliability and stability of

$$\varphi(z) = \varphi^0(z) + \varphi^{00}(z), \psi(z) = \psi^0(z) + \psi^{00}(z),$$

$$P(z,\bar{z}) = P^0(z,\bar{z}) + P^{00}(z,\bar{z}) \qquad (1)$$

where $\varphi^0(z), \psi^0(z), P^0(z,\bar{z})$ - stress functions of the main characterizing the untouched massif; $\varphi^{00}(z), \psi^{00}(z), P^{00}(z,\bar{z})$ - stress functions of the additional state caused by the presence of the structure, and $P(z,\bar{z})$ − the solution of the well-known Helmholtz equation of the form by (2) [11]:

$$\Delta P + c^2 P = 0 \qquad (2)$$

where Δ - Laplace operator, value c^2 - is the square of the modulus of the wave vector.

The Helmholtz equation is an elliptic partial differential equation that is solved using numerical methods of equations of mathematical physics [12].

Let us first consider the state of an untouched rock mass, in which an underground structure has not yet been laid, and then we will move

where $\sigma_x^0, \sigma_y^0, \tau_{xy}^0, \tau_{yx}^0 \left(\tau_{xy}^0 \neq \tau_{yx}^0\right)$ - components of normal and shear stresses of the untouched massif.

Hooke's law relates the stress and strain of an elastic medium according to formula (4):

$$\varepsilon_x^0 = \frac{1}{2G}\left[\sigma_x^0 - v\left(\sigma_x^0 + \sigma_y^0\right)\right], \quad \varepsilon_y^0 = \frac{1}{2G}\left[\sigma_y^0 - v\left(\sigma_x^0 + \sigma_y^0\right)\right],$$

$$\gamma_{xy}^0 = \frac{1}{4G}\left(\tau_{xy}^0 + \tau_{yx}^0\right) \qquad (4)$$

where $\varepsilon_x^0, \varepsilon_y^0, \gamma_{yx}^0 -$ zero strain components in the untouched massif, G is the shear modulus, and ν is Poisson's ratio.

Deformations are related to the displacement vector components by formulas (5):

$$\varepsilon_x^0 = \frac{\partial u^0}{\partial x}, \ \varepsilon_x^0 = \frac{\partial \upsilon^0}{\partial y}, \ \gamma_{xy}^0 = \frac{1}{2}\left(\frac{\partial \upsilon^0}{\partial x} + \frac{\partial u^0}{\partial y}\right) \qquad (5)$$

According to the hypothesis of A.N. Dinnik, in an untouched rock mass, a point can move vertically down [13], i by formula (6):

$$u^0 = 0, \ \upsilon^0 \neq 0 \qquad (6)$$

Then from formulas (4) we obtain the following expression for stress according to formula (7):

$$\sigma_y^0 = -\gamma H \qquad (7)$$

where γ - specific (volumetric) weight of a rock mass, H - depth of the considered array point.

Now the main stress functions will look like this (8):

$$\varphi^0(z) = \Gamma z = -\frac{\gamma H(1+\lambda)}{4} z, ,$$

$$\psi^0(z) = \Gamma' z = -\frac{\gamma H(1-\lambda)}{2} z, \ \mathrm{P}^0(z,\bar{z}) = 0 \qquad (8)$$

where $\lambda = \frac{\nu}{1-\nu}$ - side pressure coefficient, $\Gamma, \Gamma' -$ stress distribution characteristics at infinity, $\varphi^0(z)$, $\psi^0(z) -$ Kolosov-Muskhelishvili stress functions for rock massif [14].

Let a horizontal unfixed tunnel of non-circular section be laid in a homogeneous elastic isotropic rock mass at a depth H from the day surface. Such an array is modeled under plane deformation conditions as an infinite isotropic elastic weightless plane with asymmetric stress tensors. It is weakened by a hole of a given shape in the plane of the complex variable z=x+iy and free from external forces and moments, as shown in the design Figure 1.
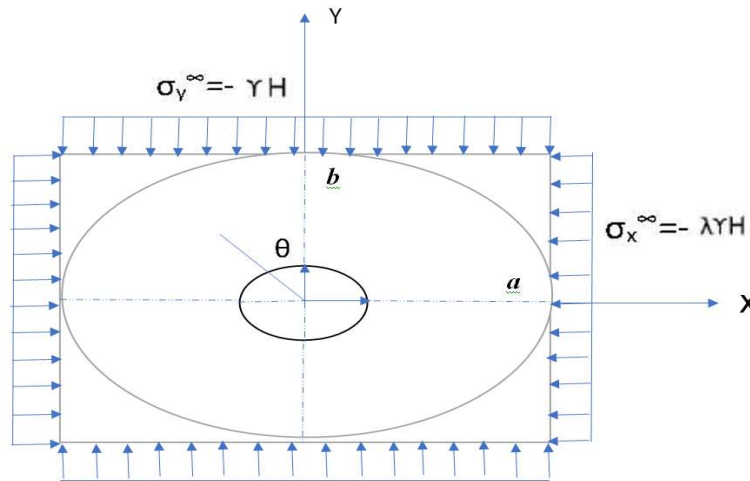

Figure 1: Calculation scheme of the problem

Using the mapping function (9), we conformally map the entire infinite region outside the hole onto the exterior of the unit circle in the plane of the complex variable $\zeta = \xi + i\eta = pe^{i\theta}$:

$$z = \omega(\zeta) = R[\zeta + \varepsilon\phi(\zeta)] \qquad (9)$$

under condition (10):

$$1 + \varepsilon\phi(\zeta) \neq 0 \ \text{ at } |\zeta| \geq 1 \qquad (10)$$

Where

$$\phi(\zeta) = \sum_1^N (\alpha_n + i\beta_n)\zeta^{-n} \ (\alpha_n, \beta_n, R - const), \ \varepsilon -$$ a small numerical parameter that is in the interval $-1 \leq \varepsilon \leq 1$ and characterizes the deviation of a given hole from a circular one.

For an elliptical hole and the mapping function for R=(a+b)/2 and ε=(a-b)/(a+b) (-1≤ε≤ 1) will look like formula (11):

For an elliptical hole $\varepsilon\phi(\zeta) \neq 0$, and the mapping function for R=(a+b)/2 and ε=(a-b)/(a+b) (-1≤ε≤ 1) will look like formula (11):

To solve the problem in the displayed area, the following conditions are set:

2. Border conditions:
- at infinity, forces equal to the forces according to formula (13) act:

$$\sigma_\xi^\infty = -\lambda\gamma H, \ \sigma_\eta^\infty = -\gamma H, \ \tau_{\xi\eta}^\infty = \tau_{\eta\xi}^\infty = 0 \tag{13}$$

- on the contour of a unit circle at according to the formula (14):

$$\sigma_\rho - i\tau_{\rho\theta} = 0 \tag{14}$$

where $\sigma_\xi^\infty, \sigma_\eta^\infty, \tau_{\xi\eta}^\infty, \tau_{\eta\xi}^\infty$, - stress components at infinity, $\sigma_\rho, \tau_{\rho\theta}$ - stress components on the circuit.

Then the main stress functions will take the following form according to formula (15):

$$\varphi^0(\zeta) = \Gamma\omega(\zeta), \psi^0(\zeta) = \Gamma'\omega(\zeta), P^0(\zeta,\overline{\zeta}) = 0 \tag{15}$$

and the functions of additional stresses are found from the boundary conditions and, according to the Laurent theorem, can be represented by uniformly convergent power series according to formula (16):

$$\varphi^{00}(\zeta) = a_n\zeta^{-n}, \psi^{00}(\zeta) = \sum_0^\infty b_n\zeta^{-n},$$

$$P^{00}(\zeta,\overline{\zeta}) = \sum_{-\infty}^\infty p_n K_n(cR\rho)e^{-in\theta} \tag{16}$$

where $K_n(cR\rho) -$ modified Bessel function of the second kind of the nth order of the imaginary argument (McDonald function) [13].

Potentials $\varphi(\zeta), \psi(\zeta), P(\zeta,\overline{\zeta})$ outside the contour of the hole will be sought in the form of series in powers of the small parameter ε according to formula (17) and we will restrict ourselves to the zeroth and first approximations:

$$z = \omega(\zeta) = R(\zeta + \varepsilon\zeta^{-1}) \tag{11}$$

1. Initial conditions at t=0 according to formula (12):

$$\upsilon_p^n = 0, \upsilon_\theta^n = 0, \omega_{p\theta}^n = 0 \tag{12}$$

$$\varphi(\zeta) = \sum_0^\infty \varepsilon^n\varphi_n(\zeta), \quad \psi(\zeta) = \sum_0^\infty \varepsilon^n\psi_n(\zeta),$$

$$P(\zeta,\overline{\zeta}) = \sum_0^\infty \varepsilon^n P_n(\zeta,\overline{\zeta}) \tag{17}$$

We expand the functions included in the boundary conditions into functional series in powers of a small parameter and compare the expressions with each other for its equal powers. For expansion, we also use the following well-known power series according to formula (18):

$$\frac{1}{(1+x)^2} = \sum_0^\infty (-1)^{k+1}kx^{k-1} = 1 - 2x + 3x^2 - \dots \tag{18}$$

After all the necessary transformations, we obtain the desired expressions (19):

$$\varphi(\zeta) = \Gamma\zeta + \frac{a_1^{(0)}}{\zeta} + \varepsilon(\frac{\Gamma}{\zeta} + \frac{a_1^{(1)}}{\zeta} + \frac{a_3^{(1)}}{\zeta^3})$$

$$\psi(\zeta) = \Gamma'\zeta + \frac{b_1^{(0)}}{\zeta} + \frac{b_3^{(0)}}{\zeta^3} + \varepsilon\left[\frac{\Gamma'}{\zeta} + \frac{b_1^{(1)}}{\zeta} + \frac{b_3^{(1)}}{\zeta^3} + \frac{b_5^{(1)}}{\zeta^5}\right]$$

$$P(\zeta,\overline{\zeta}) = \left[p_2^{(0)}e^{2i\theta} + \overline{p}_2^{(0)}e^{-2i\theta}\right]K_2(cR\rho) +$$

$$+ \varepsilon\left\{\Gamma'\frac{F}{1+F}\frac{c^2R^2}{6cK_1(cR)}K_2(cR\rho)\sin 4\theta +\right.$$

$$+ \varepsilon\left\{\left[p_2^{(1)}e^{2i\theta} + \overline{p}_2^{(1)}e^{-2i\theta}\right]K_2(cR\rho)\right.$$

$$\left.+ \left[p_4^{(1)}e^{4i\theta} + \overline{p}_4^{(1)}\right]K_4(cR\rho)\right\} \tag{19}$$

at $K_{n+1}(cR\rho) = \frac{2n}{cR\rho}K_n(cR\rho) + K_{n-1}(cR\rho)$

To find the derivatives of the function, the following well-known recursive formulas (20) were used:

$$\frac{\partial^k}{\partial \zeta^k}\Big[\mathrm{K}_n(cR\rho)e^{\pm in\theta}\Big] = \left(-\frac{cR}{2}\right)^k \mathrm{K}_{n\mp k}e^{\pm i(n\mp k)\theta},$$

$$\frac{\partial^k}{\partial \overline{\zeta^k}}\Big[\mathrm{K}_n(cR\rho)e^{\pm in\theta}\Big] = \left(-\frac{cR}{2}\right)^k \mathrm{K}_{n\pm k}e^{\pm i(n\pm k)\theta} \tag{20}$$

Equating the coefficients at the same powers σ^n (n=1,3,-1) from the first condition, at and from $\sin 2\theta$ and $\cos 2\theta$ the second condition, we obtain a system of algebraic equations for determining the unknown coefficients. Having solved it, we find that the unknown coefficients $a_1^{(0)}, b_1^{(0)}, b_3^{(0)}, p_2^{(0)}$ are equal to expressions (21):

$$a_1^{(0)} = -\frac{\Gamma'}{1+F}, \quad b_1^{(0)} = -2\Gamma, \quad b_3^{(0)} = -\frac{1-F}{1+F}\Gamma',$$

$$p_2^{(0)} = -i\frac{F}{1+F}\frac{\Gamma'}{c\mathrm{K}_1(cR)} \tag{21}$$

where the notation

$$F = \frac{8(1-\nu)}{4 + c^2R^2 + 2cR[\mathrm{K}_0(cR)/\mathrm{K}_1(cR)]}.$$

Let us now determine the stress, displacement, and rotation components in the zeroth approximation using the following substitution (22):

$$\Gamma = -\frac{\gamma H(1+\lambda)}{4}, \quad \Gamma' = -\frac{\gamma H(1-\lambda)}{2} \tag{22}$$

- for the main stress state at zero approximation of stress and displacement, we find according to formulas (23):

$$\sigma_\rho^{(0)0} = -\frac{\gamma H}{2}\big[(1+\lambda) - (1-\lambda)\cos 2\theta\big],$$

$$\sigma_\theta^{(0)0} = -\frac{\gamma H}{2}\big[(1+\lambda) + (1-\lambda)\cos 2\theta\big]$$

$$\tau_{\rho\theta}^{(0)0} = -\frac{\gamma H}{2}(1-\lambda)\sin 2\theta \tag{23}$$

$$\tau_{\theta\rho}^{(0)0} = -\frac{\gamma H}{2}(1-\lambda)\sin 2\theta,$$

$$\upsilon_\rho^{(0)0} = -\frac{\gamma H\rho}{4G}\big[(1-2\nu)(1+\lambda) - (1-\lambda)\cos 2\theta\big],$$

$$\upsilon_\theta^{(0)0} = -\frac{\gamma H\rho}{4G}(1-\lambda)\sin 2\theta,$$

- for an additional stress state at zero approximation, the values of stresses and displacements on the contour of a unit circle at ρ=1 can be found using formulas (24):

$$\sigma_\rho^{(0)00} = \frac{\gamma H}{2}\big[(1+\lambda) - (1-\lambda)\cos 2\theta\big]$$

$$\sigma_\theta^{(0)00} = -\frac{\gamma H}{2}\left[(1+\lambda) + \left[3 - \frac{4F}{1+F}\right](1-\lambda)\cos 2\theta\right]$$

$$\tau_{\rho\theta}^{(0)00} = \frac{\gamma H}{2}(1-\lambda)\sin 2\theta$$

$$\tau_{\theta\rho}^{(0)00} = \frac{\gamma H}{2}\left[1 - \frac{2F}{1+F}\left[2 + cR\frac{K_0(cR)}{K_1(cR)}\right]\right] \times$$
$$\times (1-\lambda)\sin 2\theta \tag{24}$$

$$\upsilon_\rho^{(0)00} = -\frac{\gamma H\rho}{4G}\left[\begin{array}{l}(1+\lambda) - \left[3 - 4\nu - \frac{4(1-\nu)F}{1+F}\right]\times \\ \times(1-\lambda)\cos 2\theta\end{array}\right]$$

$$\upsilon_\theta^{(0)00} = -\frac{\gamma H\rho}{4G}\left[3 - 4\nu - \frac{4(1-\nu)F}{1+F}\right](1-\lambda)\sin 2\theta$$

- the components of the main stresses and displacements at the first approximation on the working contour at ρ=1 can be found by formulas (25):

$$\sigma_\rho^{(1)0} = \frac{\gamma H(1-\lambda)}{2}\{\cos 4\theta - 1\},$$

$$\sigma_\theta^{(1)0} = -\frac{\gamma H(1-\lambda)}{2}\{\cos 4\theta - 1\},$$

$$\tau_{\rho\theta}^{(1)0} = -\frac{\gamma H(1-\lambda)}{2}\sin 4\theta, \tag{25}$$

$$\tau_{\theta\rho}^{(1)00} = -\frac{\gamma H(1-\lambda)}{2}\sin 4\theta,$$

$$\upsilon_\rho^{(1)0} = -\frac{\gamma HR}{4G}\left\{\begin{array}{l}-\frac{1-\lambda}{2} + (1+\lambda)(1-2\cos 2\theta) - \\ -\frac{1-\lambda}{2}\cos 4\theta\end{array}\right\},$$

$$\upsilon_\theta^{(1)0} = -\frac{\gamma HR}{4G}\left\{2(1+\lambda)(2\nu-1)\sin 2\theta + \frac{1-\lambda}{2}\sin 4\theta\right\}$$

Let us calculate and determine the components of stresses, displacements and rotations in the first approximation on the working contour at ρ=1 using formulas (26):

$$\sigma_\rho^{(1)00} = -\frac{\gamma H(1-\lambda)}{2}\big[\cos 2\theta - 1\big]$$

$$\sigma_\theta^{(1)00} = -\frac{\gamma H(1-\lambda)}{2} - \frac{2\gamma H(1+\lambda)}{1+F}\cos 2\theta -$$
$$-\frac{2\gamma H(1-\lambda)}{1+F}\left[\frac{3-F}{4} - \frac{4(1-\nu)R_2}{R_1}\right]\cos 4\theta$$

$$\tau_{\rho\theta}^{(1)00} = \frac{\gamma H(1-\lambda)}{2} \sin 4\theta \qquad (26)$$

$$\tau_{\theta\rho}^{(1)00} = \tau_{\rho\theta}^{(1)00} + c^2 R_1$$

at $\quad R_1 = 1 + \dfrac{96(1-v)K_3}{c^2 R^2 [K_3 + K_5]}$,

$$R_2 = \frac{K_1 - \dfrac{2}{cR}K_2}{K_1 + K_3} + \frac{\left(\dfrac{24}{c^2 R^2} - 1\right)K_3}{K_3 + K_5}, \qquad (27)$$

$$R_3 = \frac{1 + \dfrac{24}{c^2 R^2}\left[4(1-v)\dfrac{R_2}{R_1} - 1\right]}{K_3 + K_5}$$

$$R_4 = F - 1 + 4(1-v)\left\{ \begin{array}{l} \dfrac{R_2}{R_1}\left[1 - \dfrac{32(1-v)}{c^2 R^2}\right] + \\[2mm] \dfrac{R_3 K_5}{3} - \dfrac{3K_3 - K_1}{6(K_1 + K_3)} + \dfrac{8}{c^2 R^2} \end{array}\right\}$$

Stresses, displacements and rotation for the first approximation are found as the sum of the main (24) and additional (26).

The total stresses, displacements and rotations for a loose elliptical working will be obtained as the sum of the zero and first approximations (main and additional).

3. RESULT AND DISCUSSION

On the basis of the obtained theoretical formulas, we will carry out numerical calculations of stresses, deformations and displacements in the siltstone massif around an unfixed and fixed mountain structure of a transverse elliptical shape.

The initial calculated data for such a rock will be as follows: $E = 0.62 \cdot 10^{10} MPa$, $v=0.20$, $\alpha=0.726$, $\delta = 0.0094\ second^{\alpha-1}$, $\lambda=0.25$, cR=3, Macdonald functions of the second kind are: $K_0 = 0.0347$, $K_1 = 0.0402$, $K_2 = 0.0615$, $K_3 = 0.1222$, $K_4 = 0.3059$, $K_5 = 0.9378$, $K6 = 3.4318$.

The polar angle is taken in the interval $0 \le \theta \le 2\pi$.

Table 1 shows the values of the main stresses of the intact rock mass in the zero and first approximation, calculated by formulas (231) and (25) in dimensionless units.

Table 1: The main stresses of the intact rock mass in the zero and first approximation.

θ, grad	$-\dfrac{\sigma_\rho^{(0)0}}{\gamma H}$	$-\dfrac{\sigma_\rho^{(1)0}}{\gamma H}$	$-\dfrac{\sigma_\theta^{(0)0}}{\gamma H}$	$-\dfrac{\sigma_\theta^{(1)0}}{\gamma H}$	$-\dfrac{\tau_{\rho\theta}^{(0)0}}{\gamma H}$	$-\dfrac{\tau_{\rho\theta}^{(1)0}}{\gamma H}$	$-\dfrac{\tau_{\theta\rho}^{(0)0}}{\gamma H}$	$-\dfrac{\tau_{\theta\rho}^{(1)0}}{\gamma H}$
0	0.250	0.000	1.000	0.000	0.000	0.000	0.000	0.000
15	0.300	0.188	0.949	-0.188	0.188	0.325	0.188	0.325
30	0.438	0.563	0.813	-0.563	0.325	0.325	0.325	0.325
45	0.625	0.750	0.625	-0.750	0.375	0.000	0.375	0.000
60	0.813	0.563	0.438	-0.563	0.325	-0.325	0.325	-0.325
75	0.949	0.188	0.302	-0.188	0.188	-0.325	0.188	-0.325
90	1.000	0.000	0.250	0.000	0.000	0.000	0.000	0.000
105	0.949	0.188	0.302	-0.188	-0.188	0.325	-0.188	0.325
120	0.812	0.563	0.438	-0.563	-0.325	0.325	-0.325	0.325
135	0.625	0.750	0.625	-0.750	-0.375	0.000	-0.375	0.000
150	0.438	0.563	0.813	-0.563	-0.325	-0.325	-0.325	-0.325
165	0.300	0.188	0.949	-0.188	-0.188	-0.325	-0.188	-0.325
180	0.250	0.000	1.000	0.000	0.000	0.000	0.000	0.000

Figure 2 shows the main radial stresses in the zeroth and first approximation, from which it can be seen that the radial stresses in the zeroth approximation are symmetrical about the coordinate axes and the rock mass experiences only compression. The radial stress at the lateral points of the contour is 4 times less than the stresses at the upper points, and the circumferential stresses, on the contrary, are less.
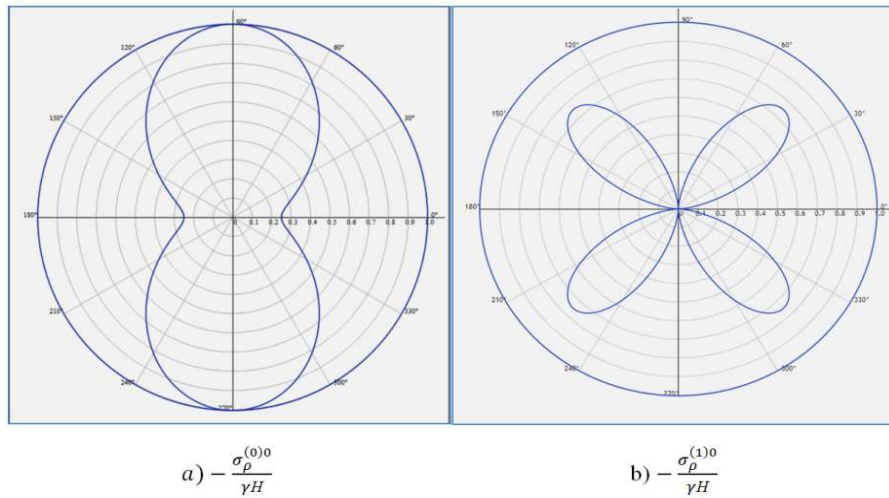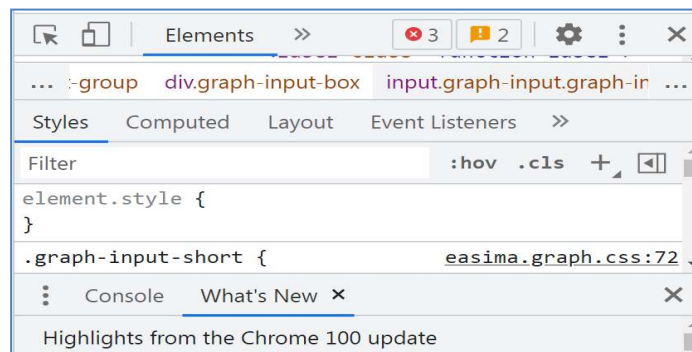
$$a) - \frac{\sigma_\rho^{(0)0}}{\gamma H} \qquad\qquad b) - \frac{\sigma_\rho^{(1)0}}{\gamma H}$$

Figure 2: Basic radial stresses in zero and first approximation

Figure 3 shows the code for the plotting program.

Figure 3: Plotting program code [http://yotx.ru/]

Figure 4 shows the main circumferential stresses in the zero and first approximation, from which it can be seen that they are symmetrical about the coordinate axes and the rock mass experiences only compression.
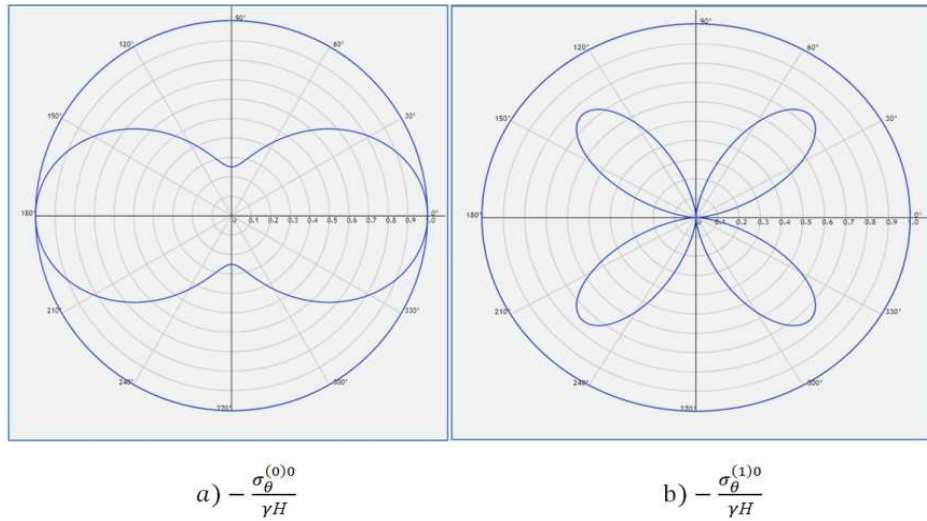
$$a) - \frac{\sigma_\theta^{(0)0}}{\gamma H} \qquad\qquad b) - \frac{\sigma_\theta^{(1)0}}{\gamma H}$$

Figure 4: Basic circumferential stresses in zero and first approximation

In the first approximation, the patterns of distribution of radial and circumferential stresses coincide, but instead of compression, the massif experiences stretching. At $\theta = 0^o, 90^o, 180^o, 270^o$, the stress values are equal to zero, and at $\theta = 45^o, 135^o, 225^o, 315^o$, the maximum values are obtained.

Figure 5 shows the main shear stresses in the zero and first approximation, from which it can be seen that they are symmetrical about the axis of the bisector of the first quarter. In this case, in the first and third quarters, the array experiences only compression, and in the rest of the area, tension. Shear stresses are symmetrical with respect to the coordinate axes, and the array alternately experiences compression and and stretching.

$$a) - \frac{\tau_{\rho\theta}^{(0)0}}{\gamma H} \qquad\qquad b) - \frac{\tau_{\rho\theta}^{(1)0}}{\gamma H}$$
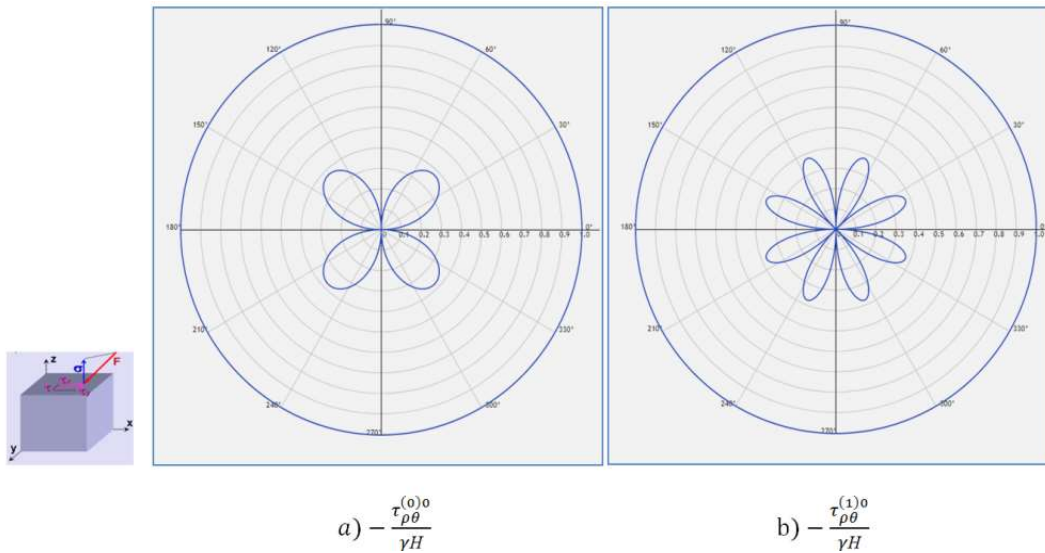
Figure 5: Basic shear stresses in zero and first approximation

Let us consider the distribution of additional stresses in the zero and first approximation in the rock mass around the loose elliptical working. Table 2 shows the values of additional stresses calculated by formulas (22) and

(24) in dimensionless units.

Table 2: Additional stresses in the rock mass around the loose elliptical working.

θ, grad	$-\dfrac{\sigma_\rho^{(0)00}}{\gamma H}$	$-\dfrac{\sigma_\rho^{(1)00}}{\gamma H}$	$-\dfrac{\sigma_\theta^{(0)00}}{\gamma H}$	$-\dfrac{\sigma_\theta^{(1)00}}{\gamma H}$	$-\dfrac{\tau_{\rho\theta}^{(0)00}}{\gamma H}$	$-\dfrac{\tau_{\rho\theta}^{(1)00}}{\gamma H}$	$-\dfrac{\tau_{\theta\rho}^{(0)00}}{\gamma H}$	$-\dfrac{\tau_{\theta\rho}^{(1)00}}{\gamma H}$
0	-0.250	0.000	1.359	2.624	0.000	0.000	0.000	0.000
15	-0.302	-0.188	1.261	2.177	-0.1885	-0.325	0.261	-0.543
30	-0.434	-0.563	0.992	1.099	-0.3258	-0.325	0.452	0.005
45	-0.625	-0.750	0.625	-0.025	-0.375	0.000	0.522	1.495
60	-0.813	-0.563	0.258	-0.749	-0.325	0.325	0.452	2.585
75	-0.949	-0.188	-0.011	-1.027	-0.188	0.325	0.261	2.038
90	-1.000	0.000	-0.109	-1.074	0.000	0.000	0.000	0.000
105	-0.949	-0.188	-0.011	-1.027	0.188	-0.325	-0.261	-2.038
120	-0.813	-0.563	0.258	-0.749	0.325	-0.325	-0.452	-2.585
135	-0.625	-0.750	0.625	-0.025	0.375	0.000	-0.522	-1.495
150	-0.437	-0.563	0.992	1.099	0.325	0.325	-0.452	-0.005
165	-0.301	-0.188	1.261	2.177	0.188	0.325	-0.261	0.5437
180	-0.250	0.000	1.359	2.624	0.000	0.000	0.000	0.000

Figure 6 shows additional radial stresses in zero and first approximation. Figure 6 shows that the pattern of distribution of radial stresses coincides with the picture for the main field, only the array is under compression.
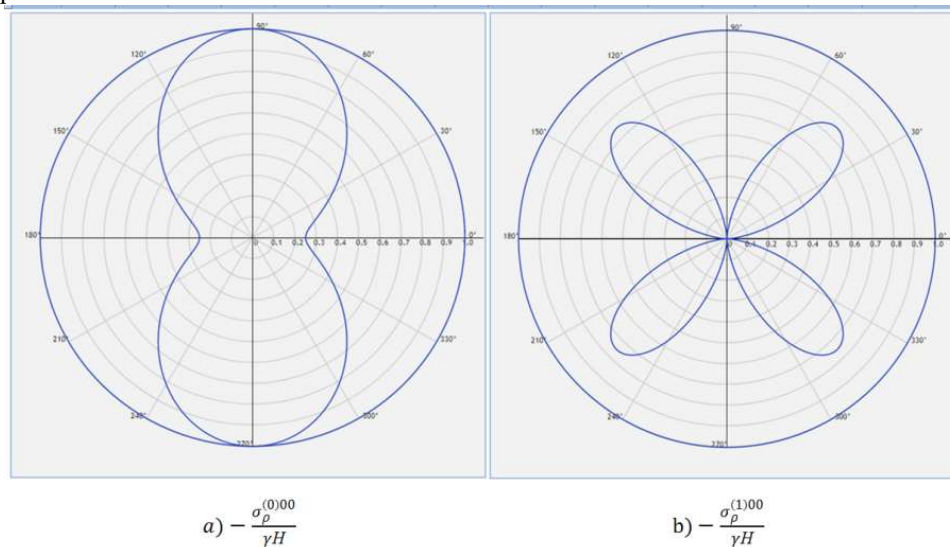

$$a) - \frac{\sigma_\rho^{(0)00}}{\gamma H} \qquad b) - \frac{\sigma_\rho^{(1)00}}{\gamma H}$$

Figure 6: Additional stresses in zero and first approximation

Figure 7 shows additional hoop stresses in the zero and first approximation. Circumferential radial stresses, in contrast to radial ones, are heterogeneous: in the upper part of the contour, an area of tensile stresses is found, and in the rest of the array is under compression. The distribution along the contour is uneven, and at the side points of the contour, the voltage is several times greater than at the upper points.

Figure 8 shows additional shear stresses in zero and first approximation.
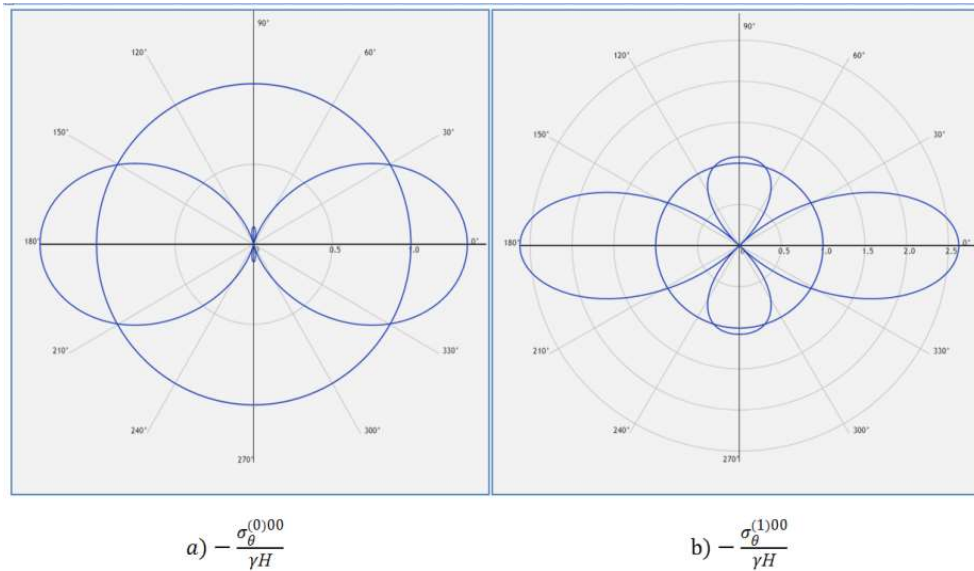
a) $-\dfrac{\sigma_\theta^{(0)00}}{\gamma H}$ b) $-\dfrac{\sigma_\theta^{(1)00}}{\gamma H}$

Figure 7: Additional circumferential stresses in zero and first approximation

a) $-\dfrac{\tau_{\rho\theta}^{(1)00}}{\gamma H}$ b) $-\dfrac{\tau_{\rho\theta}^{(1)00}}{\gamma H}$
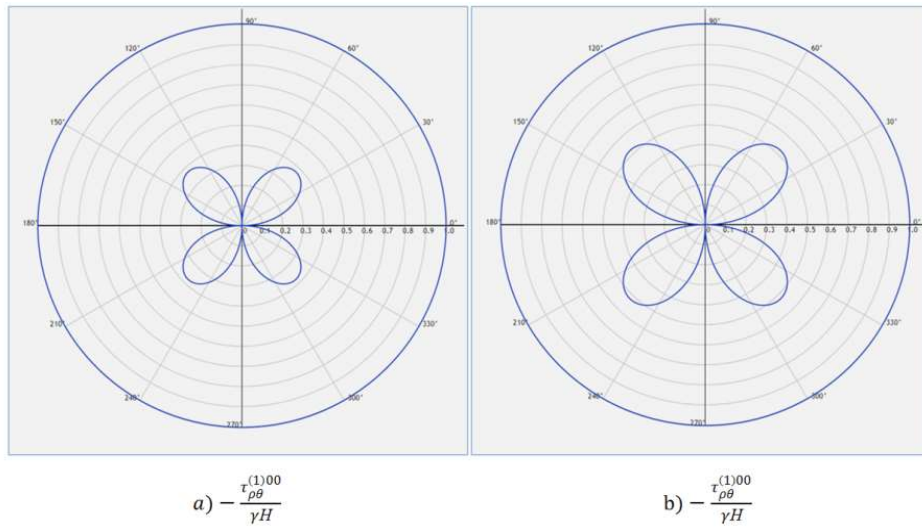
Figure 8: Additional shear stresses in zero and first approximation

The qualitative picture of the distribution of the main and additional shear stresses is the same, but differs quantitatively.

4. CONCLUSION

The obtained analytical formulas for calculating stresses in the initial elastic state and in the state due to the presence of an underground structure make it possible to determine the zones of increased concentration of impact on the structure.

Such changes occur at the critical points of the bifurcation, and then the distribution law of the quantities under study changes. In practice, this will allow engineers to identify the risks of collapse of underground structures and take preventive measures to reduce a possible man-made disaster. Such measures will help to avoid human losses and reduce the material from the occurrence of emergencies.

The advantage of this work lies in the fact that, unlike previously published works in this area of research, the authors obtained an analytical and numerical solution to the problem. In addition, a graphic representation of the stress distribution on the contour of an underground structure shows the

critical areas of bifurcations in which the structure can become unstable.

The consequence of such a process is material damage and human losses if workers were underground at that time. Identification of the risks of possible catastrophic conditions of the underground structure will allow taking preventive measures to reduce such losses and damage.

REFERENCES

[1] S.L. Castillo Daza, F. Naranjo Mayorga. Simplified Model of the Catastrophe Theory for the Landslides Study // Revista Ciencia en Desarrollo. - 2015. - Vol. 6, No. 1. – Pp. 61-65.

[2] Poincare A., Couturat L. Mathematics and Logic. - M.: LKI, 2018. - 152 p.

[3] Abdelati El Allaoui, Said Melliani and Lalla Saadia Chadli. Stability of Fuzzy Dynamical Systems via Lyapunov Functions. Hindawi Publishing Corporation //Mathematical Problems in Engineering. - 2020.

[4] Gilmore, Robert. The Topology of Chaos. Alice in Stretch and Squeezeland. WILEY-VCH, 2018. 581 p.

[5] Chengping Zhang, Kaihang Han. Collapsed Shape of Shallow Unlined Tunnels Based on Functional Catastrophe Theory. Hindawi Publishing Corporation //Mathematical Problems in Engineering. – 2015. Article ID 681257, 13 pages. Web Resource http://dx.doi.org/10.1155/2015/681257.

[6] Wei Bin Zhang. Synergetic Economics: Time and Change in Nonlinear Economics. Springer Science & Business Media. 2013. 246 p.].

[7] Murray, Stacey R. "The Rise and Fall of Catastrophe Theory". www.encyclopedia.com. Retrieved 2 November 2021.

[8] Arnold, Vladimir Igorevich. Catastrophe Theory, 3rd ed. Berlin: Springer-Verlag, 1992.

[9] Fomichev A.V. Elements of the theory of bifurcations and dynamical systems. Part 1. Moscow, MFTI, 2019. 42 p.

[10] Fomichev A.V. Elements of the theory of bifurcations and dynamical systems. Part 2. Moscow, MFTI, 2019. 50 p.

[11] Knyazev, S.Yu. Numerical solution of boundary value problems for inhomogeneous Helmholtz equations by the method of field point sources /S.Yu. Knyazev, E. E. Shcherbakova, A. N. Zaichenko//News of higher educational institutions. Electromechanics. - 2014. -№ 4. - P. 14-19.

[12] Shvartsman D.A.. Equations of mathematical physics. Alternative and new solutions. – Yustitsinform, 2021. – 238 p.

[13] Dinnik A.N. Application of Bessel functions to problems in the theory of elasticity. - Selected works. – Publisher Academy of Sciences of the Ukrainian SSR. - 1952.

[14] Muskhelishvili N.I. Some basic problems of the mathematical theory of elasticity. – M.: Nauka, 1966. – 707 p.